JGR Oceans

RESEARCH ARTICLE
10.1029/2022JC018877

Density Staircases Are Disappearing in the Canada Basin of the Arctic Ocean

Claire Ménesguen[1], Camille Lique[1], and Zoé Caspar-Cohen[1]

[1]Laboratoire d'Océanographie Physique et Spatiale, CNRS, IRD, Ifremer, University Brest, Brest, France

Key Points:

- Density staircases are detected over the past two decades in in situ observations in the Beaufort Gyre
- Density staircases have been gradually smoothed, with a transition that begins in the western part of the Canada Basin
- Smoothing of staircases occurs simultaneously with changes in the large scale dynamics

Correspondence to:

C. Ménesguen,
claire.menesguen@ifremer.fr

Citation:

Ménesguen, C., Lique, C., & Caspar-Cohen, Z. (2022). Density staircases are disappearing in the Canada Basin of the Arctic Ocean. *Journal of Geophysical Research: Oceans*, *127*, e2022JC018877. https://doi.org/10.1029/2022JC018877

Received 19 MAY 2022
Accepted 1 NOV 2022

Abstract In the Canada Basin of the Arctic Ocean, warm and salty Atlantic-origin Water (AW) lies in the intermediate layer (250–800 m) below a colder and fresher surface layer. It results in a depth range where vertical thermohaline gradients are propitious to double-diffusion. Indeed, thermohaline staircases are commonly observed and associated with double-diffusive processes. Using observations from the Beaufort Gyre Exploration Project large database and Ice-Tethered Profilers, we document the presence of density staircases in the 300–700 m depth range with a striking strong spatial and temporal coherence. However, since 2007, a progressive smoothing of these staircases has occurred, beginning from the western half of the basin. Quantifying this evolution, we find that a general pattern is a clear evolution over time from numerous thick steps (≃40 m) with sharp interfaces to fewer and thinner steps (≃30 m) with smoother interfaces. After 2014, marked density staircases have almost disappeared in most of the Canada Basin. The vanishing of staircases occurs over a few years and coincides with modifications of the large scale circulation and thermohaline large scale horizontal gradients. As the small scale thermohaline structures are thought to play an important role for the vertical and horizontal exchanges of heat within the Canada Basin, the disappearance of the steps may impact the heat distribution at depth, with potential consequences for the evolution of the sea ice cover.

Plain Language Summary In the western side of the Arctic Ocean, Atlantic-origin water lies around 400 m deep, and is warmer and saltier than the surface layer, resulting in a peculiar stratification compared to the other oceans. Moreover, the interior of this ocean is thought to be quieter than the open ocean. As a result of this unique setting, specific mechanisms based on the difference in temperature and salinity capacity to diffuse can play a role in the formation of step-like structures often observed in vertical profiles. Using observations of temperature and salinity in the western Arctic, we show that the steps are numerous, thick (≃40 m) and coherent over long time and space in 2005–2010. Yet, in recent years, the steps have started to gradually weaken and even to disappear in the western part of the Canada Basin. As the steps are thought to play an important role for the vertical and horizontal exchanges of heat within the Canada Basin, their disappearance may impact the heat distribution at depth, with potential consequences for the evolution of the sea ice cover.

1. Introduction

In the Canada Basin of the Arctic Ocean, the intermediate layer (250–800 m) is occupied by warm and salty Atlantic-origin Water (AW), which lies below a colder and fresher surface layer. As a result, in this region, temperature and salinity both increase with depth until the core of the AW layer (marked by the AW temperature maximum around 400 m; Figure 1a). Below this maximum, temperature decreases again while salinity continues to increase with depth. This peculiar setting of stratification and combination of vertical thermohaline gradients is often associated with the presence of step-like structures in temperature and salinity, whose development have been commonly linked to double-diffusive processes (see for instance the Figure 1 of van der Boog, Dijkstra, et al. (2021) for a global distribution of the presence of step-like structures). Indeed, such staircases have been observed since the 1970s in the Canada Basin. Moreover, at least two kinds of features have been reported to coexist, with different thicknesses and thermohaline characteristics (Bebieva & Timmermans, 2017).

First, thin steps (~3–10 m thick) have been observed in the depth range between ~200 m and ~350 m. Although hard to detect from in situ observations (with vertical resolution often comparable to the thickness of the step itself), these features have received a lot of attention from the Arctic science community (Neal & Neshyba, 1973; Neal et al., 1969; Padman & Dillon, 1987, 1988; Timmermans et al., 2008). They are well-mixed, producing vertical homogenization of temperature and salinity, and therefore density. Their long distance coherence has

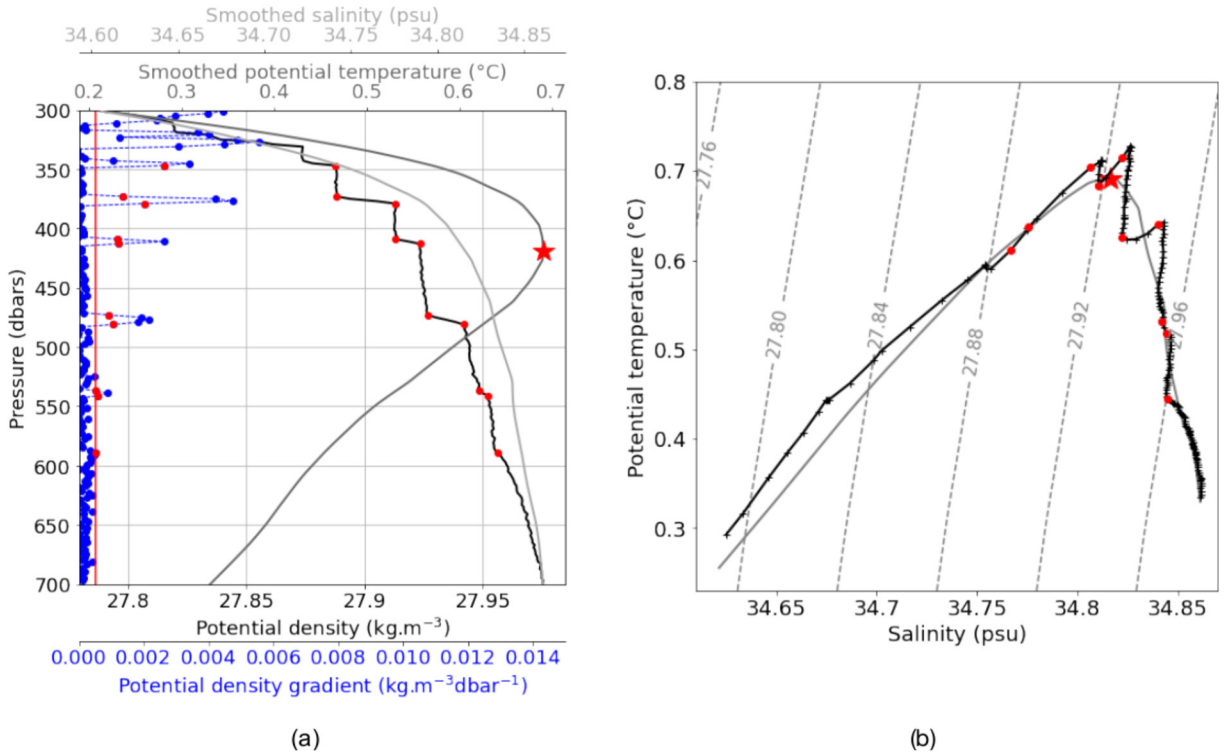

Figure 1. Vertical profiles from mooring D for a single cast in March 2007. (a) Potential temperature and salinity profiles smoothed by a 50 m rolling mean are respectively in gray and light gray. The red star indicates the AW core temperature. Density profile (black solid line) and its corresponding vertical density gradient (blue dashed line). Pairs of red dots delimit the density steps. The red solid line shows the vertical density gradient threshold delimiting the steps (b) θ-S diagram (black solid lines with markers for values every 2 dbar). Gray line is the smoothed profile with the red star indicating the AW core.

been known for decades (Padman & Dillon, 1988). More recently, based on the analysis on 3 years of measurements from Ice-Tethered Profilers (ITP, Toole et al., 2011), Timmermans et al. (2008) have revealed the persistence of the staircases throughout the Canada Basin, with a striking lateral coherence of each mixed layer across the entire basin (i.e., about 800 km). Such a spatial coherence of these thin homogeneous layers presents an uncommon aspect ratio of the order of 10^5 to 10^6. In this depth range, above the AW temperature maximum, the large scale thermohaline vertical gradients are in a configuration propitious for the Diffusive Convective (DC) double-diffusive instability (Radko, 2013; Turner & Stommel, 1964). As such, the presence of thin layers has been largely interpreted as the signature of DC instability (Neshyba et al., 1971; Padman & Dillon, 1987, 1988; Shibley & Timmermans, 2019; Shibley et al., 2017).

Second, observational studies have also highlighted the presence of thicker steps (~40–60 m thick) deeper in the water column around and below the AW temperature maximum, between ~350 m and ~650 m (Carmack et al., 1997; McLaughlin et al., 2009; Woodgate et al., 2007). These thicker steps are usually associated with temperature and salinity vertical gradients that almost compensate in density, producing characteristic zigzags in T-S diagrams around the temperature maximum (Figure 1b). McLaughlin et al. (2009) have documented their appearance within the interior of the whole Canada Basin in the early 2000s, and their further steadiness over a few years. These thicker steps have been commonly interpreted as the signature of thermohaline intrusions (Bebieva & Timmermans, 2017, 2019; Carmack et al., 1997; Perkin & Lewis, 1984), alternating over the vertical areas propitious to DC and Salt-Fingering (SF), another double-diffusive unstable regime. Intrusions are thought to be spread laterally into the basin interior from the topographically-steered AW boundary current, which propagate cyclonically along the margin of the Canada Basin (McLaughlin et al., 2009; Walsh & Carmack, 2003).

The variability in the basin-scale circulation and the associated thermohaline characteristics have most likely an impact on the occurrence of intrusions. For instance, Carmack et al. (1995, 1997) have documented a strong warming of the AW (with temperatures exceeding 1°C) during the 1990s. The warm anomaly has propagated in the southern part of the Canada Basin, and has likely resulted in the appearance of intrusions throughout the

interior of the basin. The propagation of a second warm anomaly was identified in the early 2000s by McLaughlin et al. (2009), and is thought to have been advected cyclonically along with the AW current along the continental slope and transferred toward the interior of the basin through thermohaline intrusions. More generally, the temperature within the AW layer is known to exhibit large spatio-temporal variations on decadal timescales, superimposed to a warming trend since the 1950s (Polyakov et al., 2012). Yet, it remains unclear if the presence of thermohaline intrusions throughout the basin can only occur during the warm phases of the AW temperature variability. Moreover, other large scale changes are also known to affect the properties and the circulation of the AW layer. For instance, the spin up of the surface Beaufort Gyre driven by an increase of the wind stress curl since 2008 (Giles et al., 2012; Regan et al., 2019) has resulted in both a deepening of the core of the AW (Zhong & Zhao, 2014) and a decrease in the amount of AW advected into the Canada Basin (Lique et al., 2015). It is thus timely to examine the recent evolutions of the staircases within the Canada Basin.

Here we focus on the thicker steps found between 300 and 700 m in the Canada Basin, based on the analysis of the Beaufort Gyre Exploration Project (BGEP, Proshutinsky et al., 2009, 2019) data set spanning the last two decades. More specifically, we aim to (a) highlight the temporal and spatial coherence of the thicker steps and (b) show the recent and gradual vanishing of these structures. The remainder of this paper is organized as follows. The different datasets used for the study are briefly described in Section 2. In Section 3, we examine the strong lateral coherence and temporal stability of the density steps found in the Canada Basin. We then document their gradual and recent vanishing in Section 4. The potential mechanisms associated with this disappearance are discussed in Section 5. Summary and conclusions are given in Section 6.

2. Measurements and Methods

As part of BGEP, up to four moorings have been deployed and maintained in the Canada Basin since August 2003 (Figure 2a). Each mooring carries a McLane Moored Profiler, which returns conductivity-temperature-depth (CTD) and velocity profiles between 60 and 2000 m at profiling intervals of 6 and then 48 hr (Proshutinsky et al., 2009). The processing of the data set has been performed consistently for the full record by Woods Hole Oceanographic Institution, following the procedure described in Krishfield et al. (2004). The processed data set has a vertical resolution of 2 dbar. Temperature and salinity data are expected to be measured with an accuracy of 0.01°C and 0.02 psu, respectively. Note that we only use data from three moorings (A, B, and D), which are the moorings with the longest deployment period. We also make use of the ship-based CTD measurements gathered during the annual BGEP hydrographic surveys performed every late summer in the same region (a CTD cast from the cruise in 2006 is shown as an example in Figure 2a).

Additionally, we analyze temperature and salinity profiles from 56 ITPs drifting in the Canada Basin between 2004 and 2019. ITP consists of a surface buoy deployed on an ice floe and a tether along which a CTD profiling unit measures pressure, temperature, and salinity between ∼7 m and ∼750 m depth (Krishfield, Toole, & Timmermans, 2008; Toole et al., 2011). Between two and six profiles are returned every day, meaning that two consecutive profiles are spaced by a few kilometers or less. We only make use of data that have been fully processed up to Level 3, meaning that the data have been pressure-bin averaged at 1-db vertical resolution (see reference in the Data availability statement for a full description of the processing procedure).

Throughout our study, temperature and salinity profiles from mooring, CTD cast or ITP are used to estimate density profiles. Temperature and density refer to potential temperature and potential density referenced locally, respectively.

We use the density profiles from moorings, ITPs and cruises to detect steps. Previous detections of the thinner and shallower steps in the Canada Basin were mostly based on temperature profiles (e.g., Shibley et al., 2017), while detections of thicker and deeper steps were often based on temperature-salinity ($\theta - S$) diagrams (e.g., Carmack et al., 1997; Perkin & Lewis, 1984). However, the two types of structures exhibit staircases in density profiles (see McLaughlin et al., 2009; Padman & Dillon, 1987). In order to gather all features and to exclude sharp temperature and salinity gradients compensated in density, resulting from pure isopycnal stirring, we choose to perform our detection on density profiles. As such, our method, tracking alternance of strong and weak vertical gradients of density, follows the method of van der Boog, Koetsier, et al. (2021), who have censused thermohaline staircases in the global ocean, using Argo floats and ITP data. However, in contrast to our study, they wanted to

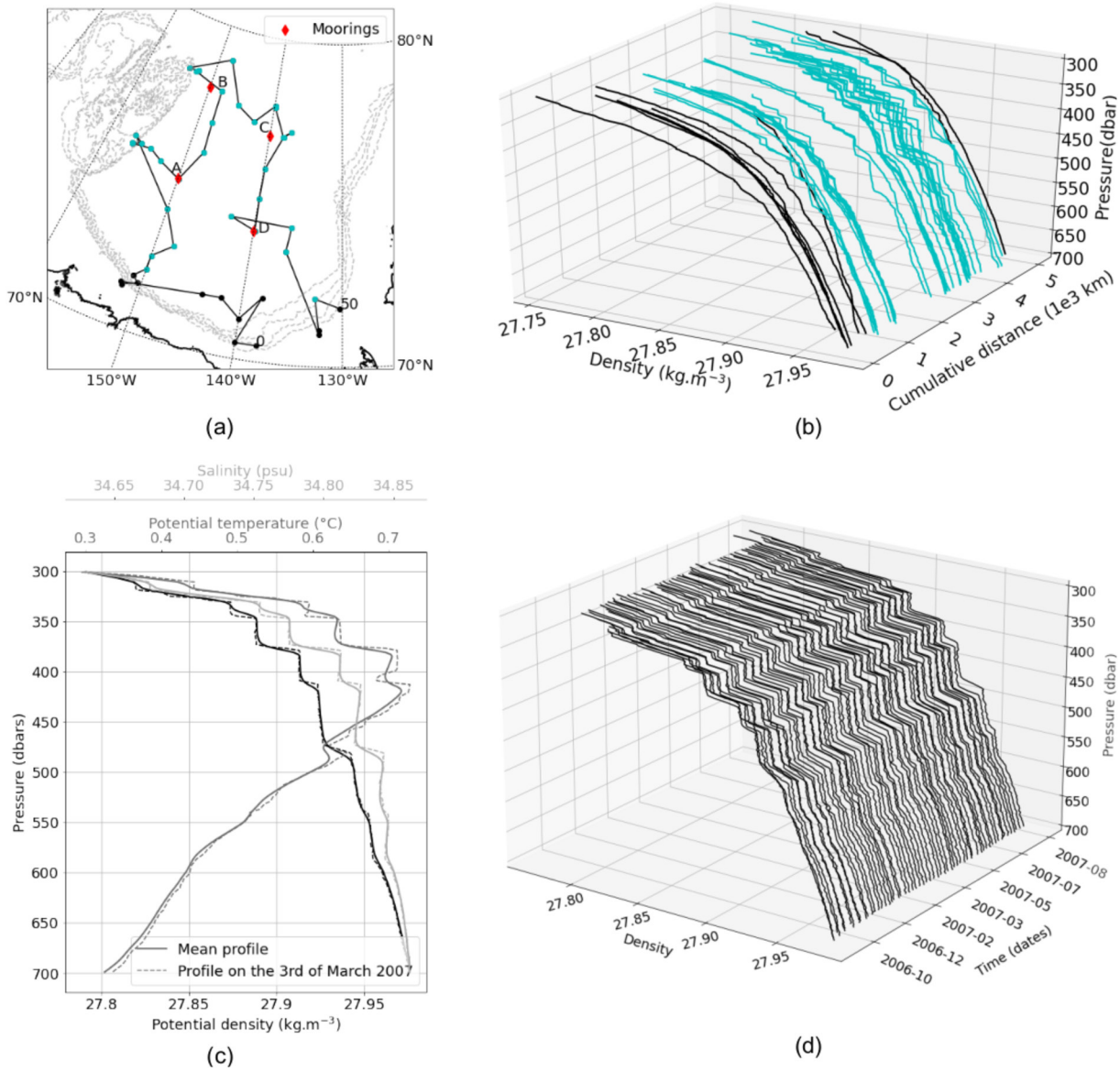

Figure 2. (a) Position of the four moorings and the 2006-cruise CTD casts. The trajectory followed during the cruise is represented by the black lines between the cast positions. First and last casts are numbered (0 and 50) on the map. Dashed gray lines indicate the bathymetry contours every 500 m between the surface and 2000 m. (b) Density profiles from the 2006 survey within the 300–700 m depth range against distance traveled from the first cast. Profiles in blue correspond to the blue dots in (a) in the interior of the basin, where staircases are detected. (c) Mean temperature, salinity and density profiles from mooring D averaged between September 2006 and August 2007 are shown with solid lines. The dashed lines show the same quantities but for a single cast in March 2007. (d) Time evolution of the density profiles at mooring D (only 1 every 5 profiles is shown to improve readability).

exclude staircases that could be the result of intrusions and thus removed steps alternating SF and DC conditions from their statistics.

Here, we define density steps as structures with thickness >10 m (meaning that each step is described by at least 4 data points in its inside) between maxima of vertical density gradient ($>5 \times 10^{-4}$ kg m^{-3} dbar^{-1}) within the depth range of 300–700 m in the Canada Basin. An example of our step detection on one profile is shown in Figure 1a, where a pair of red dots delimits the selected step in the density profile (black line), and indicates the corresponding value of density gradient (blue line). Density gradients are stronger between the shallowest steps than between the deepest ones, ranging from 5×10^{-3} kg m^{-4} to 5×10^{-4} kg m^{-4}. In contrast, the density gradient within the steps is quasi-null within the shallowest steps, while it reaches small values within the deepest ones (up to 2×10^{-4} kg m^{-4}). For this reason, choosing a criterion for the sharp density gradient between steps is more

efficient to localize the steps than a criterion on the density gradient within the steps. Our detection algorithm mainly detects the larger steps (the so-called intrusions), that are particularly visible between 350 and 650 m, although we acknowledge that a few well-mixed smaller steps that are also present in the depth range we consider (300–700 m) can also be detected. Overall, our results are only showing little sensitivity to the precise choice made regarding the different thresholds.

Additionally, we define temperature and associated pressure of the AW core as the maximum temperature detected within the same depth range (300–700 m) and the pressure at which the maximum is found. As the presence of steps can biais the detection of the AW core, a vertical rolling mean with a 50-m window is applied to all profiles prior to the detection (Figure 1a).

3. Spatial and Temporal Coherence of the Density Staircases

We start by focusing on 1 year of observations (2006–2007), when intrusions are largely present in the basin (McLaughlin et al., 2009). The long term evolution of these features is addressed in detail in the following section.

The CTD profiles gathered during the August–September 2006 survey provides us with an overview of the whole Canada Basin (Figure 2a). Figure 2b reveals the presence of density staircases in most of the profiles from the basin interior. Most profiles exhibit 4–5 steps that are around 40–50 m thick. The few smoothed profiles (in black) are located close to the Alaskan continental slope, leaving the Canada basin interior and the northwestern continental shelf around the Chukchi plateau with density profiles showing density staircases aligned over several hundreds of kilometers. This spatial distribution is coherent with the schematic view of the mean AW circulation presented by Woodgate et al. (2007), revealing a AW branch characterized by the presence of thermohaline zigzags penetrating the Canada Basin north of the Chukchi Plateau, and then propagating along the Chukchi slope.

Examining the observations from mooring D between September 2006 and August 2007 reveals that the strong spatial coherence of the staircases across the basin also translates into a salient temporal coherence (Figure 2d). Over the full year, the steps remain at constant depths and exhibit nearly constant properties (e.g., their thickness or the density gradient across their interfaces). The staircases are so stable in time and depth that they are still very clearly marked in an annual mean profile (solid lines in Figure 2c), and very similar to the steps detected in a single cast in March 2007 (dashed lines in Figure 2c).

Insights on the thermohaline structures of observed density staircases can also be gained from Figure 2c. As expected, the shallower density staircases (above 350 m) are thin (a few meters) and are associated with well-mixed temperature and salinity vertical profiles. Around the AW temperature maximum and below, sharp density gradients delimit thicker steps (30–50 m). Below 400 m, they are associated with non-zero temperature and salinity gradients, which result in the striking zigzag signal around the temperature maximum in a T-S diagram (as shown later in Figure 5c). Overall, the density gradient between the steps decreases strongly with depth, by up to an order of magnitude (from 5×10^{-3} kg m^{-4} to 5×10^{-4} kg m^{-4}).

Density staircases are also visible when examining profiles from moorings A and B over the same time period, although staircases at the location of mooring B tend to be less sharp than those seen at mooring D (Figure 3 for mooring B). The time-depth evolution of the velocity profiles at mooring B exhibits three periods of strong anomalies during the same 1-year period (Figure 3b), which are the signature of mid-depth eddies passing by the location of the mooring. They are identified with velocity magnitudes greater than 15 cm s^{-1}, consistently with the eddy detection performed by Zhao and Timmermans (2015). During the illustrated 1-year period, the density profiles corresponding to the profiles during the passage of these three eddies are colored in red in Figure 3a. Statistically, they represent only 2.65% of all profiles at mooring B. Some of those profiles still show density staircases, although the depth of the steps can be slightly shifted from the ones found in the background field. Zhao and Timmermans (2015) found that eddies are more frequently observed at mooring B than at the locations of the other moorings (likely because of the proximity of mooring B with the Chukchi plateau). The disturbance by the eddies probably explains why the steps are overall less sharp at mooring B than they are at mooring D. Yet, it is remarkable that the steps are stable enough to survive the passage of eddies either locally reformed or quickly rebuilt from the background state, suggesting that their formation/maintenance mechanism plays a first order role in the dynamics and/or occur at a larger scale than the perturbations induced by the passage of eddies with the associated shear velocities. It has also been reported that steps can be observed within the core of eddies

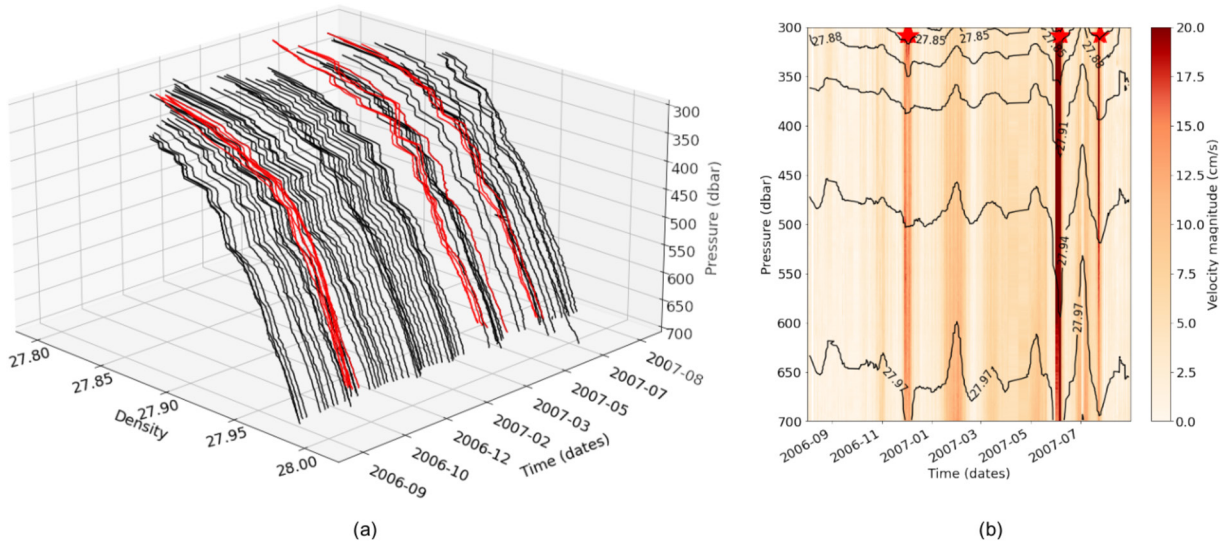

Figure 3. (a) Density profiles from mooring B between September 2006 and August 2007. Profiles in red indicate the passage of mid depth eddies. (b) Velocity magnitude from September 2006 to August 2007 from mooring B. Black lines indicate isopycnal contours. Mid depth eddies are associated with velocity magnitudes greater than 15 cm s^{-1} (spotted at the top of the panel with red stars). In February, the upper part of a deeper eddy is visible in the 300–700 m depth range with velocity magnitude smaller than 15 cm s^{-1}.

in the Canada Basin (Bebieva & Timmermans, 2016), but the impact of these very localized steps (that remains only for a short period of time close the mooring location) on the background stratification is most likely very small and beyond the scope of this paper.

Despite the very strong coherence in space and time of density staircases within the whole basin in the first year of the data record, a transition has occurred since 2005, beginning in the western side of the Canada Basin. In the following section, we will document these long-term spatio-temporal variations.

4. Gradual Vanishing of the Density Staircases

When considering a longer period of time, it appears that these thick staircases are only intermittently present in the Canada Basin. The last appearance between 1993 and 2007 was documented by McLaughlin et al. (2009). Here, we document the evolution of the density staircases in the subsequent period, during which a progressive vanishing of the staircases occurs. We first examine the density profiles from moorings A, B and D during the first and last year available for each mooring (Figures 4a, 4c and 4e). Overall, a clear transition can be seen at the three locations, with well-defined staircases visible in the first year at each mooring (2003–2004 for A and B, 2005–2006 for D) but no or smoother staircases in the last year (2016–2017 for A, 2017–2018 for B and D). We characterize the time evolution over 2003–2019 of the staircases at the mooring location based on three quantities: (a) the thickness of well-mixed steps, (b) the steepness of the slope in between two well-mixed steps and (c) the number of steps (Figures 4b, 4d and 4f). At each mooring, an obvious evolution can be seen over time, with a shift from numerous thick steps (≃40 m) with sharp interfaces to fewer and thinner steps (≃30 m) with smoother interfaces. We also indicate the standard deviation of each quantity for each year, showing that observed trends are larger than the variance of data.

The transition resulting in the vanishing of the steps is gradual throughout the Canada Basin. At moorings A and B, situated on the western side of the basin, the transition occurs earlier in the time period, in 2008–2009 for mooring A and 2012–2013 for mooring B. Meanwhile, on the eastern side of the basin at mooring D, the transition is less abrupt, and marked interfaces are still visible in 2017–2018. The slope of the step interfaces there is indeed more than twice larger than the slope of the interfaces found at A and B moorings at the end of the transition. This suggests that the transition toward a state without staircases is most likely not fully achieved at this location in 2018.

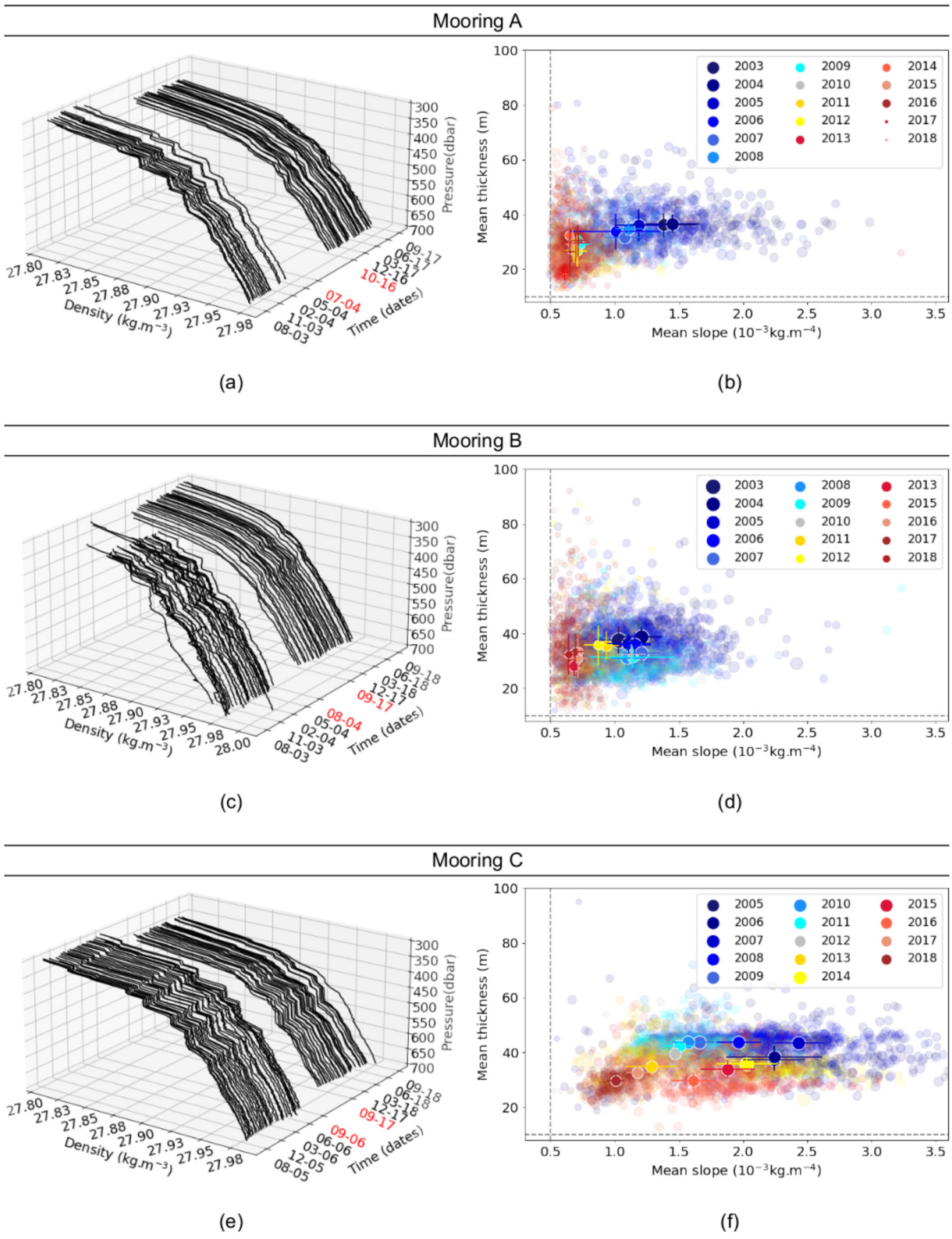

Figure 4. Density profiles at moorings A (a), B (c) and D (e) from 300 to 700 m. Only the profiles of the first year and the last year of data available for each mooring are shown. In each case, 1 every 10 profiles is shown. (b, d, and f) are scatter plots of step characteristics (mean thickness and slope between steps) for moorings A, B, and D, respectively. The size of the dots is proportional to the number of steps detected. The transparent dots indicate all the profiles while the ones with no transparency represent the mean over a year. The length of the error bars indicates the standard deviation of each quantity. We only show years during which 10 or more profiles are available. Thresholds are in gray dash lines.

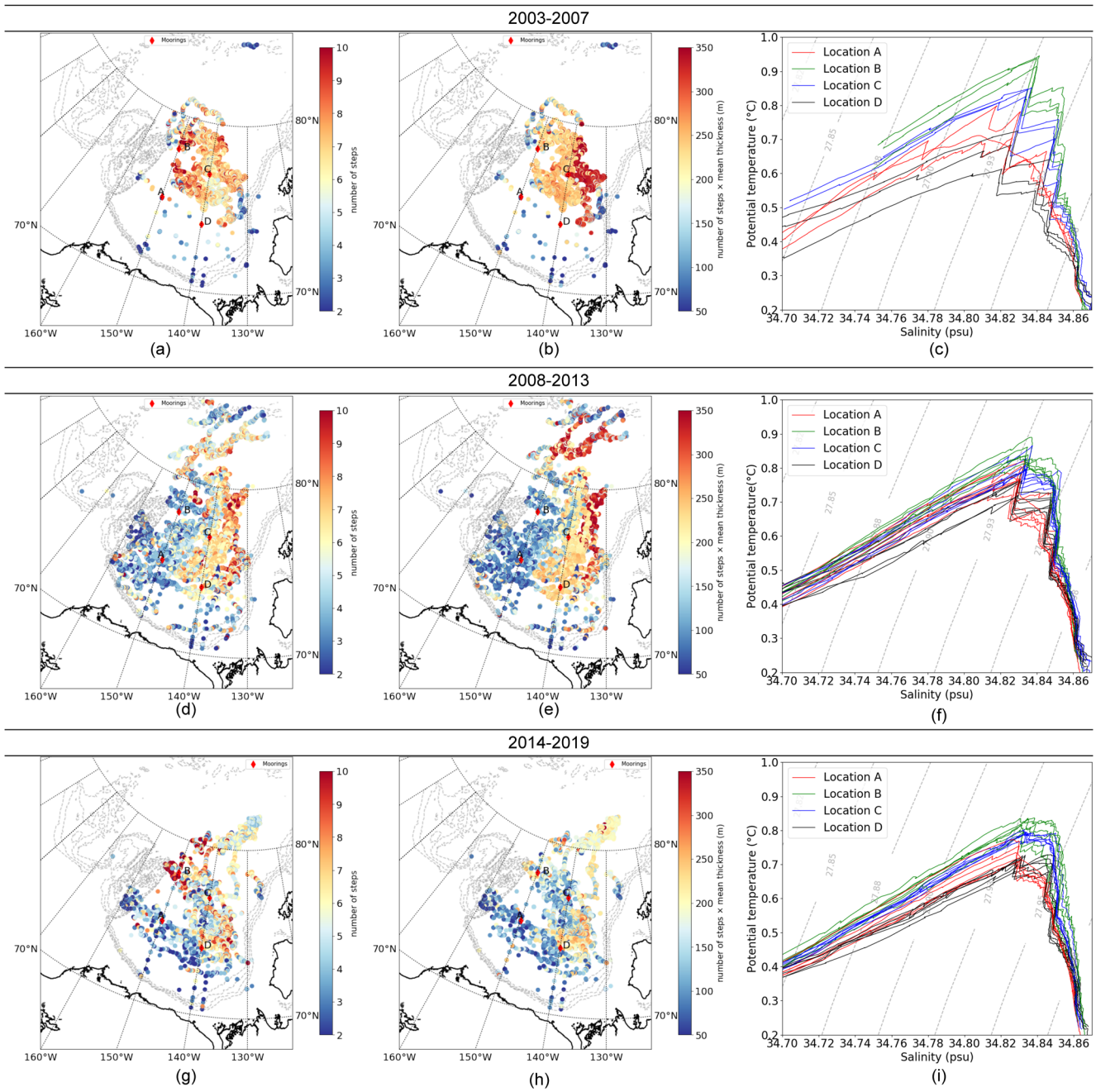

Figure 5. Maps of the number of steps (a, d, g) and the integrated thickness of the steps between 300 and 700 m depth (b, e, h, in m) for each density profile, measured by ITP or ship-based CTD casts, and θ-S diagrams for the CTD casts performed during the BGEP cruises at the mooring locations (c, f, i), for three distinct periods (2003–2007 for a, b and c, 2008–2013 for (d, e, and f) and 2014–2019 (g, h, and i).

The transition is thus not uniform over the basin. In order to gain further insight into the spatial pattern of the transition, we cluster all the data points available from ITP and ship-based CTD casts used to detect the presence of staircases (Figure 5). Here we contrast three time periods: (a) 2003–2007 when the staircases were found to spread across the Canada Basin (McLaughlin et al., 2009), (b) 2008–2013 when the transition starts to happen and (c) 2014–2019 which is representative of a new and different state. Simultaneously, we also characterize the changes affecting the large scale conditions in stratification by examining the distribution of the AW temperature maximum and the depth at which it is found over the same three time periods (Figure 6).

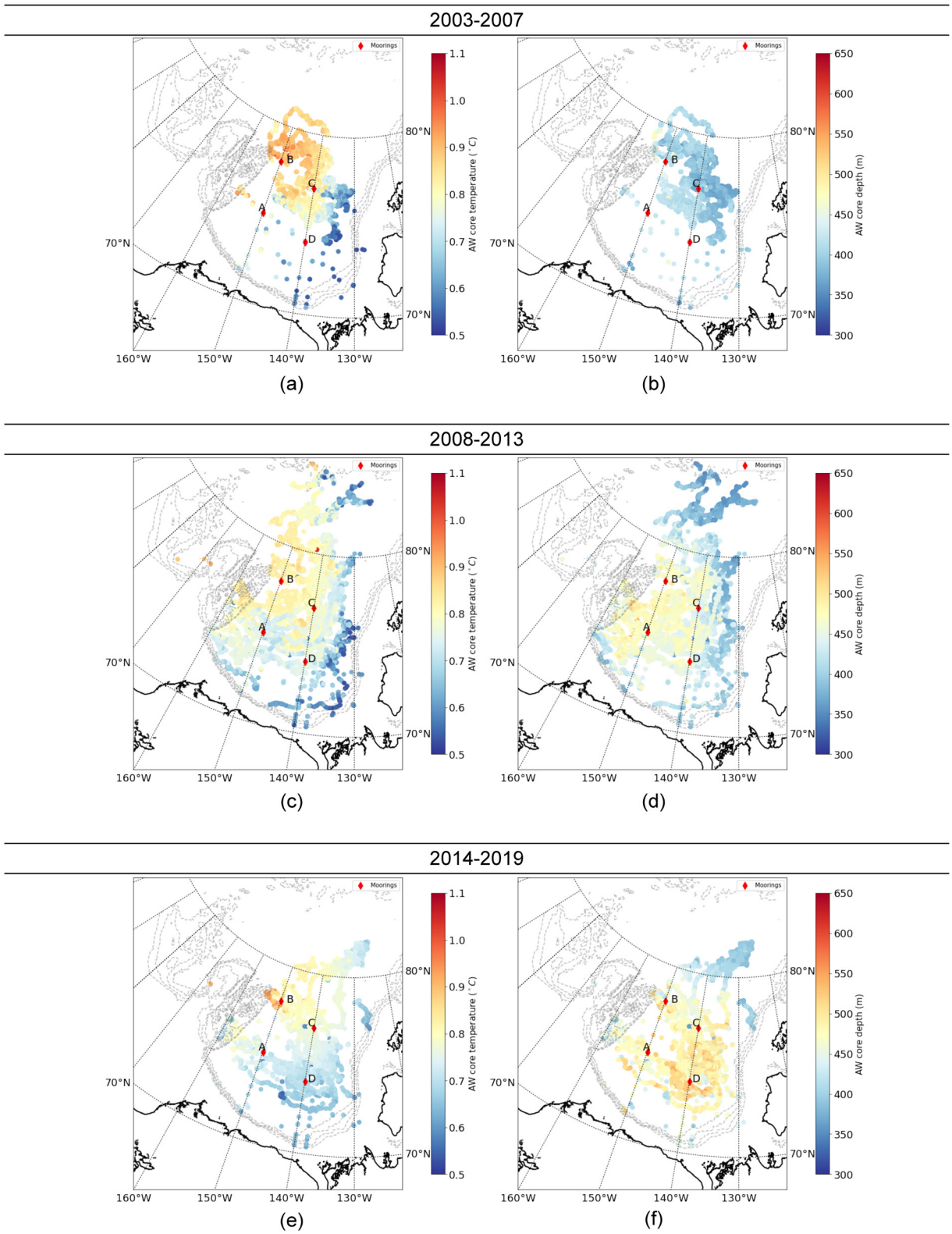

Figure 6. Maps of the AW core temperature maximum (a, c, e, in °C) and the pressure at which the maximum is found (b, d, f, in dbars) for the 2003–2007 period (a-b-c), 2008–2013 period (d-e-f) and 2014–2019 period (g-h-i). Note that each temperature profile is smoothed with a 50 m rolling mean prior to the detection of the maximum.

Between 2003 and 2007, staircases are present everywhere in the interior of the basin, and they are numerous (up to 7–8 steps per profile in the northern area; Figure 5a) and thick (up to 50 m; not shown). The integrated thickness of steps estimated from each profile reaches as high as 300 m, revealing that the staircase signal is predominant over the depth range 300–700 m in the whole basin, with an east-west gradient and a stronger signal in the eastern part of the basin (Figure 5b). During this period, $\theta - S$ diagrams display strong zigzag around the AW temperature maximum at the locations of the four moorings (Figure 5c), similar to what was observed by McLaughlin et al. (2009) over the same period. They linked these features with the propagation of a warm anomaly within the AW intermediate layer, arising from the North-Eastern part of the Chukchi plateau (Li et al., 2020). During that period, the AW temperature maximum is around 0.9°C and lies around 400 m throughout the basin, consistent with this propagation pattern.

Between 2008 and 2013, there is a clear distinction between the western and eastern parts of the basin, as expected from the evolution of the density profiles at the three moorings (Figure 4). Staircases are very scarce in the western half part of the basin (Figure 5d) and their thickness also decreases west of approximately 145°W (not shown). This results in a significant decrease of the integrated thickness of steps in the western area (divided by 2 compared to the 2003–2007 period). In the eastern area, this quantity remains large (Figure 5e). This contrast between the different parts of the basin is also seen in the $\theta - S$ diagrams, where profiles at the mooring D still exhibit clear zigzag during that period (Figure 5f). The gradual disappearance of the steps also coincides with a cooling (down to 0.8°C) and a deepening (reaching around 500 m) of the AW core beginning in the western part of the basin (Figures 6c and 6d). As a consequence of the AW core evolution, the large scale lateral gradient of temperature and salinity at the depth of the AW core decreases in the northwestern part of the basin (Figures A1 and A2).

After 2014, staircases and their associated potential temperature and salinity signature tend to disappear in most of the Canada Basin. The AW core continues to cool and deepen, reaching 0.75°C at 550 m in the eastern part of the basin (Figures 6e and 6f). The large scale gradients of temperature and salinity between the side and the center of the Canada Basin also continue to decrease (Figures A1 and A2). Most ITP and CTD casts do not exhibit staircases anymore across the 300–700 m depth range (Figures 5g and 5h), and the $\theta - S$ diagrams shows only little evidence of marked zigzag (Figure 5i). Consequently, heat fluxes between steps are expected to decrease because they are directly dependent on the temperature difference between steps (Polyakov et al., 2019).

5. Discussion

The gradual vanishing of the density staircases raises the question of mechanisms associated with the formation and maintenance of these staircases. Although we acknowledge that it remains extremely difficult to fully unravel these processes solely based on the analysis of observations, here we discuss the possible mechanisms at play.

A classical methodology to investigate the potential for double-diffusive processes to develop is to compute the Turner angle (Tu), estimated as $Tu = \tan^{-1}\left(\frac{\alpha\theta_z + \beta S_z}{\alpha\theta_z - \beta S_z}\right)$ with θ the Conservative Temperature, S, the Absolute Salinity, α and β the coefficients of thermal expansion and salinity contraction, respectively. The calculation is made with the Gibbs SeaWater Python library based on the thermodynamic equations of McDougall et al. (2009). Figure 7 shows the time-depth evolution of the Turner angle estimated from the mooring observations. In theory, in the absence of any shear, the necessary condition for the development of linear instability resulting in DC is associated with Turner angles lower than −45°. This occurs overall above the AW core, where temperature and salinity both increase with depth, creating a stratification specific to polar regions. Indeed, as noticed by van der Boog, Dijkstra, et al. (2021) (their Figure 1), the occurrence of staircases associated with a stratification propitious to a DC regime is largely confined to the polar regions. The mechanism of the instability is firstly due to a differential diffusion of heat and salt within a small interface. Convection cells are then generated above and below this sharp interface (Radko, 2013; Turner & Stommel, 1964; Veronis, 1965). However, the effect of planetary rotation, turbulent mixing, and background shear on DC staircases formation and evolution is still an open question. A review was done by Kelley et al. (2003) to gather field observations, laboratory experiments, numerical simulations and theoretical studies on the subject. More recently, Radko (2013) demonstrated that, for DC, linear theory predicts positive growth rates only in a very small part of the Tu parameter space (between −90° and −86.26°). This is only 8.3% of the full diffusive sector (between −90° and −45°). Moreover, the subsequent convection is no longer within the linear approximation and it remains difficult to associate the instability

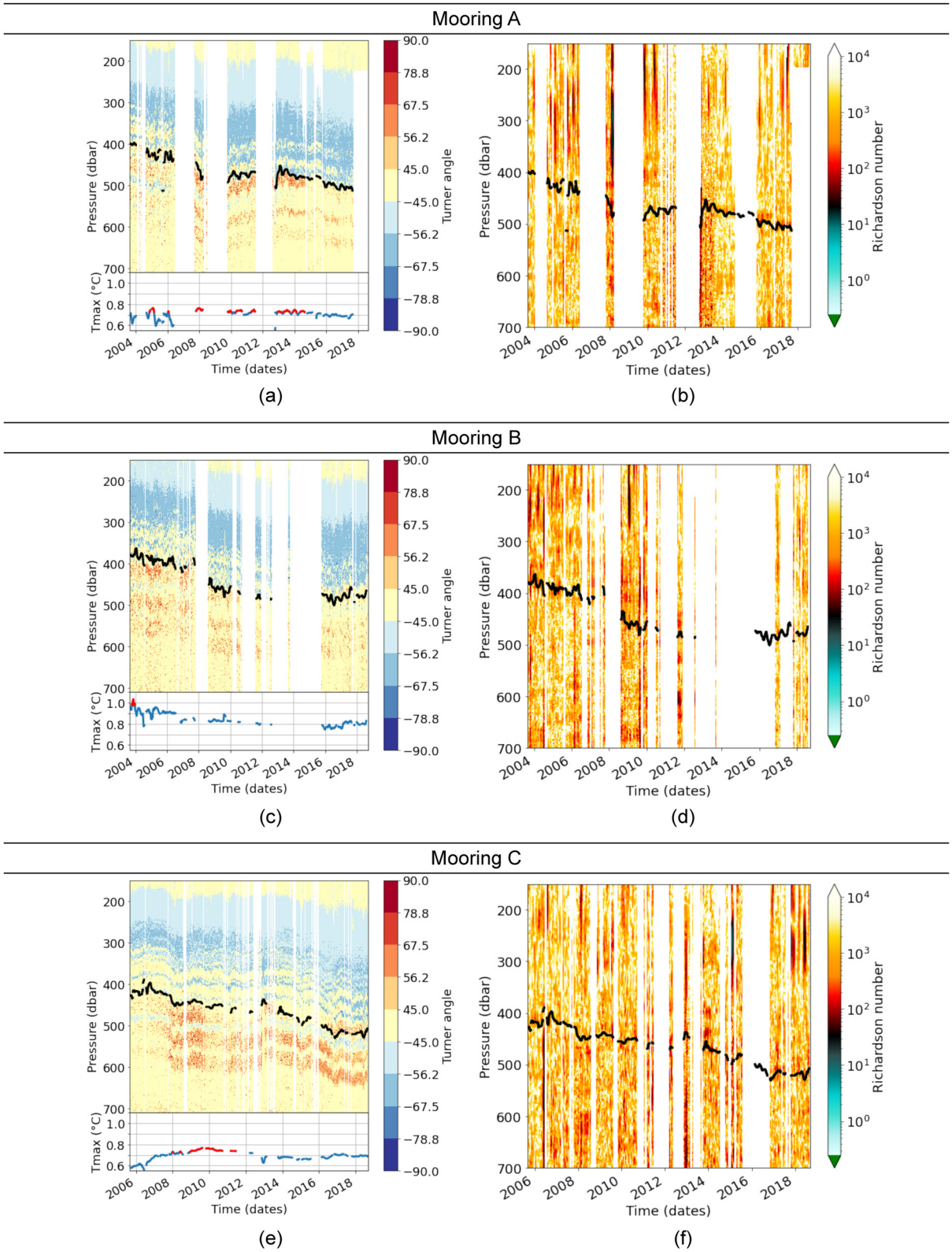

Figure 7. Hoevmoller diagrams (time-depth) of Turner angle and Richardson number for mooring A (a, b), B (c, d) and D (e, f) between 150 to 700 m. In a, c and e, orange and red colors correspond to the salt-finger regime, while blue colors indicate the diffusive sector of double-diffusion. In b, d and f, darker color and blue are for low Richardson number, and green should evidence Ri < 1/4 but never occurs in any panel. Black line corresponds to the depth of the AW core temperature maximum (note that each temperature profile is smoothed with a 50 m rolling mean prior to the detection of the maximum). The time series in a, c and e indicate the AW core temperature maximum, with red showing their highest values.

with an equilibrated state and a finite staircase generation. Some studies have aimed to tackle this issue. For example, the nonlinear evolution of a diffusive regime in the presence of a small velocity shear is studied exhaustively in Radko (2016). They found that for a Turner angle in the diffusive sector, the velocity shear widened the parameter space where the flow becomes unstable. In this case, clear, 10 m thick, thermohaline staircases can be generated, but the arrest of this vertical merging and the long term evolution are not fully elucidated as yet. The evolution of a diffusive regime is also discussed in Ma and Peltier (2022a); Ma and Peltier (2022b). They use parameterizations from stratified-turbulence of effective turbulent diapycnal diffusivities for heat and salt. In the case of salinity-dominated stratification and low-energy turbulence environment, they are able to reproduce a thermohaline-turbulence instability creating persisting staircases. But, once again, the arrest of the vertical merging is not yet fully elucidated.

In contrast, when both temperature and salinity decrease with depth, resulting in Turner angle larger than 45° characteristics of the SF regime (Figures 7a, 7c and 7e), thermohaline staircases are associated with a stratification propitious to the SF regime and are the most commonly observed step-like structures over the global ocean (van der Boog, Dijkstra, et al., 2021, their Figure 1).

Around the depth of the AW core, where we found most of our thicker steps, Figures 7a, 7c and 7e reveal that Tu is alternating between the DC and the SF sectors. At each mooring, the time when AW reaches its highest temperature is also the time when the stratification alternates more clearly over the vertical between the two sectors. As such, at Mooring A, between 2010 and 2015, Tu shows a clear vertical alternance between the DC and SF sectors. At mooring B, the alternance disappears after 2012, which also coincides with a cooling of the AW core and a decrease of the large scale temperature and salinity lateral gradients between the interior and slope of the Canada Basin, across the Beaufort Gyre (Figures A1 and A2). At mooring D, where steps are observed throughout the observational period, the alternance is particularly marked after 2008 and until the end of the time series.

Over the depth range of the AW core, similar thick steps were described by May and Kelley (2002), and were thought to be the signature of double-diffusive intrusions at the edge of the AW boundary current flowing along the slope. Such steps could indeed result from a linear phase when intrusions are exponentially growing due to the combination of a large scale thermohaline front and double-diffusive processes: vertically alternating motions across a thermohaline front lead to regions propitious to SF under warmer and saltier layers and to DC under colder and fresher layers (May & Kelley, 1997). Both double-diffusion mechanisms lead to downward density flux that converges and create a positive feed-back to the initial perturbation, driving interleaving motions and producing sharp vertical thermohaline gradients in between relatively homogeneous steps. For a more complete description, the reader should refer to Ruddick and Kerr (2003) who discuss the main theories explaining the growth and evolution of thermohaline intrusions. Yet, it is worth noticing that, here again, the non-linear equilibration, that can occur at scales several orders of magnitude larger than the initial instability perturbation, remains to be understood.

Beyond the thermohaline properties of the water column, several studies have emphasized that the vertical velocity shear could also have an effect on the linear phase of the growth of intrusions (see Ruddick & Kerr, 2003, and references therein). In order to investigate this hypothesis, we estimate the Richardson number (Ri) at the mooring, as $Ri = \overline{N}^2/\overline{u}_z^2$, with N the Brunt-Väisälä frequency, u_z the norm of the vertical derivative of the velocity. The overline stands for the large scale characteristics with a rolling average over 30 days and 60 m in depth. Ri never decreases below 1/4, meaning that shear instability is not expected to occur at those scales. Yet, the presence of shear (when $Ri \simeq 10$) suggests the triggering of thermohaline-shear instability (Radko, 2016), that can generate staircases. However, events where Richardson number is around 30 (darker areas in Figures 7b, 7d and 7f) in the 300–400 m depth range appear to occur at the different mooring as the number of observed staircases decreases: between 2006 and 2008 for mooring A, around 2010 for mooring B and later and shallower for mooring D. This observation is consistent with the observations of Bebieva and Timmermans (2016) where steps are not observed where a geostrophic Richardson number is relatively small.

6. Conclusion

In this study, we have documented the temporal and spatial evolution of the thick, density steps found around the AW temperature maximum in the Canada Basin, and have highlighted a recent transition toward their disappearance. In contrast to most previous studies that were based on the examination of temperature and salinity

characteristics, we have based our analysis on density profiles. Thus, we have selected thicker steps, englobing mainly intrusion-like features but also a few of the thickest so-called DC steps. We choose to not separate these two types of step in order to examine the occurrence of a succession of noticeable sharp vertical density gradients forming density staircases that are around 20–60 m thick in a more generic way. Focusing on the thicker steps, which are thought to be the signature of thermohaline intrusions, we have shown that they have shifted from being very stable and widespread to having almost entirely disappeared in recent years in the Canada Basin. From 2003 to 2005, steps are observed almost everywhere in the interior of the basin, and exhibit a large temporal but also spatial coherence. Surprisingly, their interactions with eddy passing by only mildly disturb them and do not destroy them in the long term. It denotes that steps are able to persist or to possibly rebuild quickly, even when strong shears occur in the velocity field at the depth of the propagating eddy passing by the mooring occasionally. After 2006, density profiles become progressively smoother, and the thickness of steps decreases, with a transition that begins in the southwestern region of the Canada Basin. The attenuation of the steps is observed further north in 2012–2013 until it reaches the southeastern part of the basin in 2017–2018. It would be interesting to investigate further if the thinner, shallower steps (resulting mainly from SF) described extensively by Shibley et al. (2017) have followed a similar evolution over the recent period in the Canada Basin, given that the presence of the deeper steps was recently suggested to affect the development of the thinner steps found upper in the water column (Shibley & Timmermans, 2022).

Overall, the appearance of the thicker, deeper staircases has been interpreted by McLaughlin et al. (2009) as a response to a warm anomaly of AW propagating primarily with the AW boundary current, establishing a large scale horizontal temperature gradient between the boundary and the interior of the basin. They suggested, however, that in the absence of this large scale thermal forcing, staircases would progressively dissipate. Here, we have documented a cooling and deepening of the AW core and a related decrease of the large scale temperature gradient beginning during the 2008–2013 period, likely resulting from the abrupt spin up of the Beaufort Gyre described by Regan et al. (2019). It is not fully clear, however, if the disappearance of the steps is indeed directly due to a disturbance of the large scale temperature gradient and the subsequent step dissipation, or to the advection of colder water to the interior of the basin, with properties that are less propitious to the development of staircases. A direct attribution remains difficult from observations, as these two large scale mechanisms would occur on similar timescales. Yet, in both cases, the occurrence of density staircases could be cyclic and directly linked to a low frequency variability of the intermediate AW layer in the Arctic Ocean on time scales of 50–80 years (Polyakov et al., 2004).

Beyond these two hypotheses for the appearance of staircases, the changing shear environment could also have an impact. In the context of a mesoscale eddy (Bebieva & Timmermans, 2016), observed a synchronicity between low Richardson number and a low step index. At the scale of the Canada Basin, we have also found time periods when the Richardson number is low within the staircases depth range, which were corresponding to the beginning of the local smoothing of steps. It remains to determine if a shear instability of the background field (when Ri is low) could be responsible for smoothing the existing staircases.

Finally, the recent smoothing of the staircases could potentially result from an increase of the turbulent mixing, arising as a possible consequence of the sea ice decline (Dosser et al., 2021). Yet, based on the analysis of mooring A data, Fine and Cole (2022) found that, over the past 15 years, in response to the sea ice decline, the estimated turbulent mixing between 50 and 300 m did not increase, despite an increase of the near-inertial energy. This is because waves are forced with large vertical wavelength, and consequently have low vertical shear. It is thus unlikely that an increased turbulent mixing would have caused the staircases to vanish.

The fate and variations of the heat stored at depth with the AW layer has been scrutinized by the Arctic science community, as it might play a role for the maintenance and evolution of the sea ice cover (Turner, 2010). In the Arctic interior, where the levels of vertical mixing and associated diffusive vertical heat flux are very low (Lique et al., 2014; Rainville & Winsor, 2008), the thin, shallow DC staircases are thought to contribute significantly to the total vertical heat flux from the warm AW layer toward the surface (Polyakov et al., 2019; Shibley et al., 2017). In contrast, the thicker, deeper, intrusion-type steps examined in this paper are thought to play a role for the transfer of heat from the boundary current to the interior of the basin (Rudels et al., 2009), diffusing laterally heat and salt, and their recent disappearance could induce variations of heat content in the interior.

However, changes of the temperature and density gradients between the boundary and the interior of the basin would also likely induce changes of the generation of eddies along the boundary current (Lique et al., 2015;

Regan et al., 2020), which are also thought to play a key role for the transfer of heat to the interior of the basin (Spall, 2013). Disentangling the relative roles and contributions of the different processes at play for the variability of the AW layer heat content would require the use of numerical models that are able to accurately simulate processes with rather unusual aspect ratio, meaning that the small scale steps would have to be simulated at the scale of the full basin. This is a great challenge for future modeling exercises focusing on the Arctic Basin.

Appendix A: Large Scale Lateral Gradient

Figures A1 and A2 illustrate a decrease over time of the large scale temperature and salinity lateral gradients between the interior and slope of the Canada Basin, across the Beaufort Gyre.

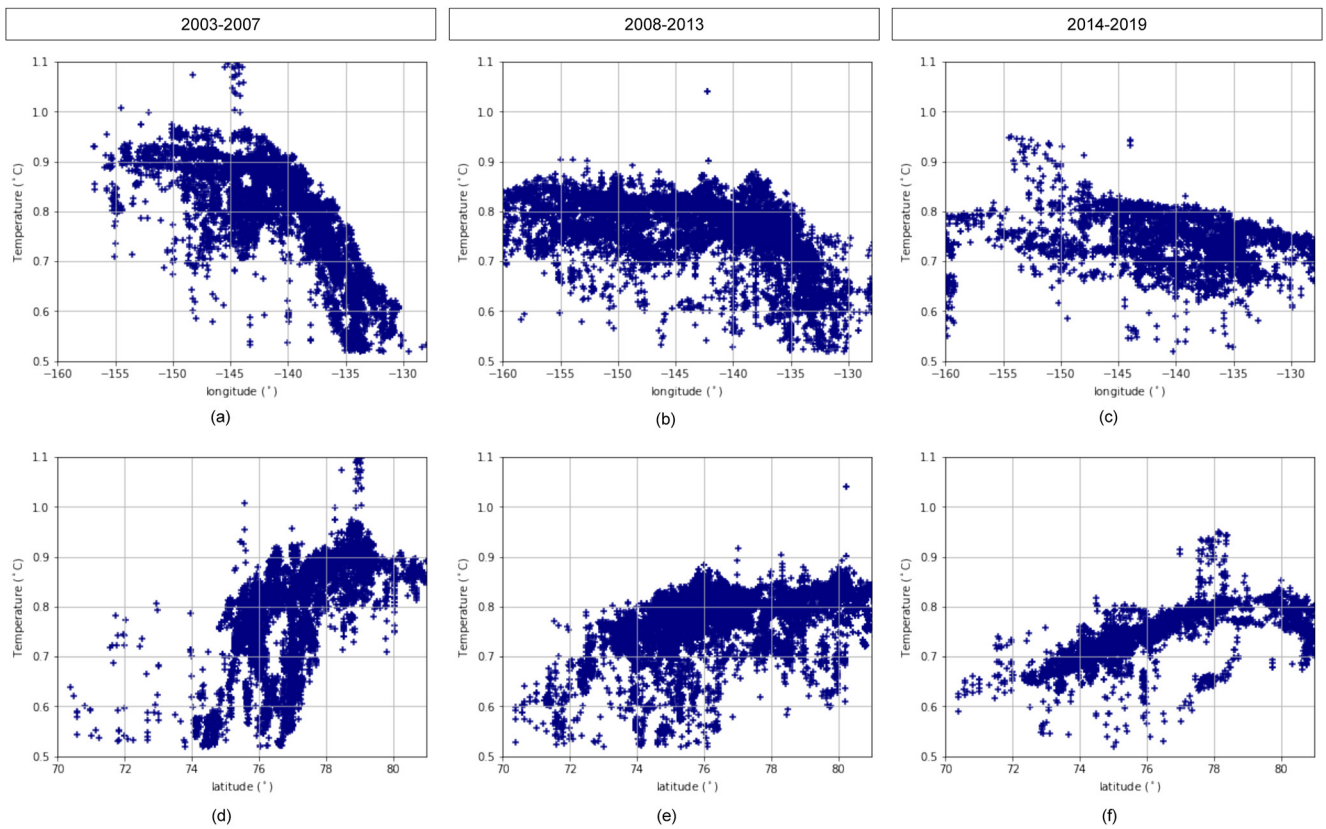

Figure A1. Scatter plots from ITP data and ship-based CTD casts of the AW core temperature maximum versus longitude (a, b, c) and latitude (d, e, f) for the 2003–2007 period (a, d), 2008–2013 period (b, e) and 2014–2019 period (c, f).

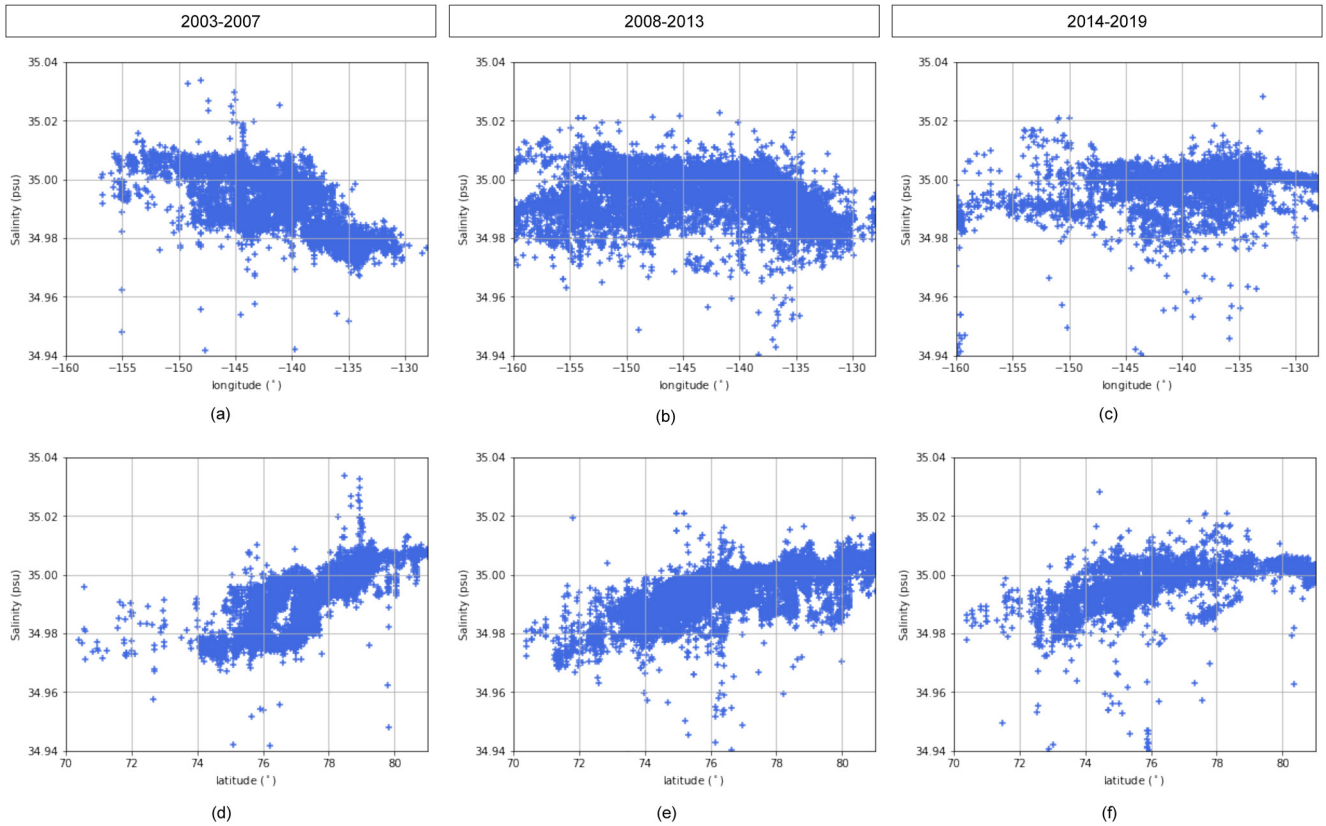

Figure A2. Scatter plots from ITP data and ship-based CTD casts of the salinity at the AW core versus longitude (a, b, c) and latitude (d, e, f row) for the 2003–2007 period (a, d), 2008–2013 period (b, e) and 2014–2019 period (c, f).

Data Availability Statement

The data were collected and made available by the Beaufort Gyre Exploration Program based at the Woods Hole Oceanographic Institution in collaboration with researchers from Fisheries and Oceans Canada at the Institute of Ocean Sciences. The Ice-Tethered Profiler data were collected and made available by the Ice-Tethered Profiler Program (Krishfield, Toole, Proshutinsky, & Timmermans, 2008; Toole et al., 2011) based at the Woods Hole Oceanographic Institution. Each data set is publicly available in post-processed form at https://www.whoi.edu/beaufortgyre and http://www.whoi.edu/itp. A notebook is given as an example of detection of steps on ITP profiles at https://www.umr-lops.fr/Le-Laboratoire/Contacts/Pages-perso/Claire-Menesguen.

Acknowledgments
This work was supported by the Routes vers lA DIssIpation and DIssipation Des tOurbillons et des oNdes internes dans l'océan projects (INSU-LEFE-IMAGO). We thank John Toole and Rick Krishfield who have kindly read a previous version of the manuscript. We also thank Timour Radko who encouraged us to finalize this study. We thank Leo Middleton and an anonymous reviewer for their very constructive comments.

References

Bebieva, Y., & Timmermans, M.-L. (2016). An examination of double-diffusive processes in a mesoscale eddy in the Arctic Ocean. *Journal of Geophysical Research: Oceans*, *121*(1), 457–475. https://doi.org/10.1002/2015jc011105

Bebieva, Y., & Timmermans, M.-L. (2017). The relationship between double-diffusive intrusions and staircases in the Arctic Ocean. *Journal of Physical Oceanography*, *47*(4), 867–878. https://doi.org/10.1175/jpo-d-16-0265.1

Bebieva, Y., & Timmermans, M.-L. (2019). Double-diffusive layering in the Canada Basin: An explanation of along-layer temperature and salinity gradients. *Journal of Geophysical Research: Oceans*, *124*(1), 723–735. https://doi.org/10.1029/2018jc014368

Carmack, E. C., Aagaard, K., Swift, J. H., MacDonald, R. W., McLaughlin, F. A., Jones, E. P., et al. (1997). Changes in temperature and tracer distributions within the Arctic Ocean: Results from the 1994 Arctic Ocean section. *Deep Sea Research Part II: Topical Studies in Oceanography*, *44*(8), 1487–1502. https://doi.org/10.1016/s0967-0645(97)00056-8

Carmack, E. C., Macdonald, R. W., Perkin, R. G., McLaughlin, F. A., & Pearson, R. J. (1995). Evidence for warming of Atlantic water in the southern Canadian Basin of the Arctic Ocean: Results from the Larsen-93 expedition. *Geophysical Research Letters*, *22*(9), 1061–1064. https://doi.org/10.1029/95gl00808

Dosser, H., Chanona, M., Waterman, S., Shibley, N., & Timmermans, M.-L. (2021). Changes in internal wave-driven mixing across the Arctic Ocean: Finescale estimates from an 18-year pan-Arctic record. *Geophysical Research Letters*, *48*(8), e2020GL091747. https://doi.org/10.1029/2020gl091747

Fine, E. C., & Cole, S. T. (2022). Decadal observations of internal wave energy, shear, and mixing in the western Arctic Ocean. *Journal of Geophysical Research: Oceans*, *127*(5), e2021JC018056. https://doi.org/10.1029/2021jc018056
Giles, K. A., Laxon, S. W., Ridout, A. L., Wingham, D. J., & Bacon, S. (2012). Western Arctic Ocean freshwater storage increased by wind-driven spin-up of the Beaufort Gyre. *Nature Geoscience*, *5*(3), 194–197. https://doi.org/10.1038/ngeo1379
Kelley, D., Fernando, H., Gargett, A., Tanny, J., & Özsoy, E. (2003). The diffusive regime of double-diffusive convection. *Progress in Oceanography*, *56*(3–4), 461–481. https://doi.org/10.1016/s0079-6611(03)00026-0
Krishfield, R., Toole, J., Proshutinsky, A., & Timmermans, M.-L. (2008). Automated ice-tethered profilers for seawater observations under pack ice in all seasons. *Journal of Atmospheric and Oceanic Technology*, *25*(11), 2091–2105. https://doi.org/10.1175/2008jtecho587.1
Krishfield, R., Toole, J. M., & Proshutinsky, A. (2004). *BGFE 2003-2004 MMP EMCTD and ACM data processing procedures*. Woods Hole Oceanographic Institution. Retrieved from https://www2.whoi.edu/site/BeaufortGyre/data/mooring-data/mooring-data-description
Krishfield, R., Toole, J. M., & Timmermans, M.-L. (2008). *ITP data processing procedures* (Vol. 24). Woods Hole Oceanographic Institution.
Li, J., Pickart, R. S., Lin, P., Bahr, F., Arrigo, K. R., Juranek, L., & Yang, X.-Y. (2020). The Atlantic water boundary current in the Chukchi borderland and southern Canada Basin. *Journal of Geophysical Research: Oceans*, *125*(8), e2020JC016197. https://doi.org/10.1029/2020jc016197
Lique, C., Guthrie, J. D., Steele, M., Proshutinsky, A., Morison, J. H., & Krishfield, R. (2014). Diffusive vertical heat flux in the Canada Basin of the Arctic Ocean inferred from moored instruments. *Journal of Geophysical Research: Oceans*, *119*(1), 496–508. https://doi.org/10.1002/2013jc009346
Lique, C., Johnson, H. L., & Davis, P. E. (2015). On the interplay between the circulation in the surface and the intermediate layers of the Arctic Ocean. *Journal of Physical Oceanography*, *45*(5), 1393–1409. https://doi.org/10.1175/jpo-d-14-0183.1
Ma, Y., & Peltier, W. (2022a). Thermohaline staircase formation in the diffusive convection regime: A theory based upon stratified turbulence asymptotics. *Journal of Fluid Mechanics*, *931*, R4. https://doi.org/10.1017/jfm.2021.945
Ma, Y., & Peltier, W. R. (2022b). Thermohaline-turbulence instability and thermohaline staircase formation in the polar Oceans. *Physical Review Fluids*, *7*(8), 083801. https://doi.org/10.1103/PhysRevFluids.7.083801
May, B. D., & Kelley, D. E. (1997). Effect of baroclinicity on double-diffusive interleaving. *Journal of Physical Oceanography*, *27*(9), 1997–2008. https://doi.org/10.1175/1520-0485(1997)027<1997:eobodd>2.0.co;2
May, B. D., & Kelley, D. E. (2002). Contrasting the interleaving in two baroclinic Ocean fronts. *Dynamics of Atmospheres and Oceans*, *36*(1–3), 23–42. https://doi.org/10.1016/s0377-0265(02)00023-4
McDougall, T., Feistel, R., Millero, F., Jackett, D., Wright, D., King, B., et al. (2009). The international thermodynamic equation of seawater 2010 (TEOS-10): Calculation and use of thermodynamic properties. In *Global ship-based repeat hydrography manual* (p. 14). IOCCP.
McLaughlin, F. A., Carmack, E. C., Williams, W. J., Zimmermann, S., Shimada, K., & Itoh, M. (2009). Joint effects of boundary currents and thermohaline intrusions on the warming of Atlantic water in the Canada Basin, 1993–2007. *Journal of Geophysical Research*, *114*(C1), C00A12. https://doi.org/10.1029/2008jc005001
Neal, V. T., & Neshyba, S. (1973). Microstructure anomalies in the Arctic Ocean. *Journal of Geophysical Research*, *78*(15), 2695–2701. https://doi.org/10.1029/jc078i015p02695
Neal, V. T., Neshyba, S., & Denner, W. (1969). Thermal stratification in the Arctic Ocean. *Science*, *166*(3903), 373–374. https://doi.org/10.1126/science.166.3903.373
Neshyba, S., Neal, V. T., & Denner, W. (1971). Temperature and conductivity measurements under ice island t-3. *Journal of Geophysical Research*, *76*(33), 8107–8120. https://doi.org/10.1029/jc076i033p08107
Padman, L., & Dillon, T. M. (1987). Vertical heat fluxes through the Beaufort sea thermohaline staircase. *Journal of Geophysical Research*, *92*(C10), 10799–10806. https://doi.org/10.1029/jc092ic10p10799
Padman, L., & Dillon, T. M. (1988). On the horizontal extent of the Canada Basin thermohaline steps. *Journal of Physical Oceanography*, *18*(10), 1458–1462. https://doi.org/10.1175/1520-0485(1988)018<1458:otheot>2.0.co;2
Perkin, R., & Lewis, E. (1984). Mixing in the west spitsbergen current. *Journal of Physical Oceanography*, *14*(8), 1315–1325. https://doi.org/10.1175/1520-0485(1984)014<1315:mitwsc>2.0.co;2
Polyakov, I. V., Alekseev, G. V., Timokhov, L. A., Bhatt, U. S., Colony, R. L., Simmons, H. L., et al. (2004). Variability of the intermediate Atlantic water of the Arctic Ocean over the last 100 years. *Journal of Climate*, *17*(23), 4485–4497. https://doi.org/10.1175/jcli-3224.1
Polyakov, I. V., Padman, L., Lenn, Y.-D., Pnyushkov, A., Rember, R., & Ivanov, V. V. (2019). Eastern Arctic Ocean diapycnal heat fluxes through large double-diffusive steps. *Journal of Physical Oceanography*, *49*(1), 227–246. https://doi.org/10.1175/jpo-d-18-0080.1
Polyakov, I. V., Pnyushkov, A. V., & Timokhov, L. A. (2012). Warming of the intermediate Atlantic water of the Arctic Ocean in the 2000s. *Journal of Climate*, *25*(23), 8362–8370. https://doi.org/10.1175/jcli-d-12-00266.1
Proshutinsky, A., Krishfield, R., Timmermans, M.-L., Toole, J., Carmack, E., McLaughlin, F., et al. (2009). Beaufort Gyre freshwater reservoir: State and variability from observations. *Journal of Geophysical Research*, *114*(C1), C00A10. https://doi.org/10.1029/2008jc005104
Proshutinsky, A., Krishfield, R., Toole, J., Timmermans, M.-L., Williams, W., Zimmerman, S., et al. (2019). Analysis of the Beaufort Gyre freshwater content in 2003–2018. *Journal of Geophysical Research: Oceans*, *124*(12), 9658–9689. https://doi.org/10.1029/2019jc015281
Radko, T. (2013). *Double-diffusive convection*. Cambridge University Press.
Radko, T. (2016). Thermohaline layering in dynamically and diffusively stable shear flows. *Journal of Fluid Mechanics*, *805*, 147–170. https://doi.org/10.1017/jfm.2016.547
Rainville, L., & Winsor, P. (2008). Mixing across the Arctic Ocean: Microstructure observations during the Beringia 2005 expedition. *Geophysical Research Letters*, *35*(8), L08606. https://doi.org/10.1029/2008GL033532
Regan, H. C., Lique, C., & Armitage, T. W. K. (2019). The Beaufort Gyre extent, shape, and location between 2003 and 2014 from satellite observations. *Journal of Geophysical Research: Oceans*, *124*(2), 844–862. https://doi.org/10.1029/2018JC014379
Regan, H. C., Lique, C., Talandier, C., & Meneghello, G. (2020). Response of total and eddy kinetic energy to the recent spinup of the Beaufort Gyre. *Journal of Physical Oceanography*, *50*(3), 575–594. https://doi.org/10.1175/JPO-D-19-0234.1
Ruddick, B., & Kerr, O. (2003). Oceanic thermohaline intrusions: Theory. *Progress in Oceanography*, *56*(3–4), 483–497. https://doi.org/10.1016/s0079-6611(03)00029-6
Rudels, B., Kuzmina, N., Schauer, U., Stipa, T., & Zhurbas, V. (2009). Double-diffusive convection and interleaving in the Arctic Ocean–distribution and importance. *Geophysica*, *45*(1–2), 199–213.
Shibley, N. C., & Timmermans, M.-L. (2019). The formation of double-diffusive layers in a weakly-turbulent environment. *Journal of Geophysical Research: Oceans*, *124*(3), 1445–1458. https://doi.org/10.1029/2018jc014625
Shibley, N. C., & Timmermans, M.-L. (2022). The Beaufort Gyre's diffusive staircase: Finescale signatures of Gyre-scale transport. *Geophysical Research Letters*, *49*(13), e2022GL098621. https://doi.org/10.1029/2022GL098621
Shibley, N. C., Timmermans, M.-L., Carpenter, J. R., & Toole, J. M. (2017). Spatial variability of the Arctic Ocean's double-diffusive staircase. *Journal of Geophysical Research: Oceans*, *122*(2), 980–994. https://doi.org/10.1002/2016jc012419

Spall, M. A. (2013). On the circulation of Atlantic water in the Arctic Ocean. *Journal of Physical Oceanography*, *43*(11), 2352–2371. https://doi.org/10.1175/jpo-d-13-079.1

Timmermans, M.-L., Toole, J. M., Krishfield, R. A., & Winsor, P. (2008). Ice-tethered profiler observations of the double-diffusive staircase in the Canada Basin thermocline. *Journal of Geophysical Research*, *113*(C1), C00A02. https://doi.org/10.1029/2008jc004829

Toole, J. M., Krishfield, R. A., Timmermans, M.-L., & Proshutinsky, A. (2011). The ice-tethered profiler: Argo of the Arctic. *Oceanography*, *24*(3), 126–135. https://doi.org/10.5670/oceanog.2011.64

Turner, J. S. (2010). The melting of ice in the Arctic Ocean: The influence of double-diffusive transport of heat from below. *Journal of Physical Oceanography*, *40*(1), 249–256. https://doi.org/10.1175/2009JPO4279.1

Turner, J. S., & Stommel, H. (1964). A new case of convection in the presence of combined vertical salinity and temperature gradients. *Proceedings of the National Academy of Sciences of the United States of America*, *52*(1), 49–53. https://doi.org/10.1073/pnas.52.1.49

van der Boog, C. G., Dijkstra, H. A., Pietrzak, J. D., & Katsman, C. A. (2021). Double-diffusive mixing makes a small contribution to the global Ocean circulation. *Communications Earth & Environment*, *2*(1), 1–9.

van der Boog, C. G., Koetsier, J. O., Dijkstra, H. A., Pietrzak, J. D., & Katsman, C. A. (2021). Global dataset of thermohaline staircases obtained from argo floats and ice-tethered profilers. *Earth System Science Data*, *13*(1), 43–61. https://doi.org/10.5194/essd-13-43-2021

Veronis, G. (1965). On finite amplitude instability in thermohaline convection. *Journal of Marine Research*, *23*(1), 1–17.

Walsh, D., & Carmack, E. (2003). The nested structure of Arctic thermohaline intrusions. *Ocean Modelling*, *5*(3), 267–289. https://doi.org/10.1016/s1463-5003(02)00056-2

Woodgate, R. A., Aagaard, K., Swift, J. H., Smethie, W. M., Jr., & Falkner, K. K. (2007). Atlantic water circulation over the Mendeleev ridge and Chukchi borderland from thermohaline intrusions and water mass properties. *Journal of Geophysical Research*, *112*(C2), C02005. https://doi.org/10.1029/2005JC003416

Zhao, M., & Timmermans, M.-L. (2015). Vertical scales and dynamics of eddies in the Arctic Ocean's Canada Basin. *Journal of Geophysical Research: Oceans*, *120*(12), 8195–8209. https://doi.org/10.1002/2015jc011251

Zhong, W., & Zhao, J. (2014). Deepening of the Atlantic water core in the Canada Basin in 2003–2011. *Journal of Physical Oceanography*, *44*(9), 2353–2369. https://doi.org/10.1175/jpo-d-13-084.1